Slab stress field in the Hellenic subduction zone as inferred from intermediate-depth earthquakes

S. Rontogianni[1], K. I. Konstantinou[1], N. S. Melis[2], and C. P. Evangelidis[2]

[1]*Institute of Geophysics, National Central University, 300 Jhongda Rd, Jhongli, 320 Taiwan*
[2]*Institute of Geodynamics, National Observatory of Athens, POB 20048, 11810 Athens, Greece*

(Received October 19, 2010; Revised November 23, 2010; Accepted November 25, 2010; Online published February 28, 2011)

The stress regime across the Hellenic subduction zone was investigated by performing stress inversion on 100 intermediate-depth moment tensor solutions. In this study, the slab was divided into four sectors based on earthquake distribution, trench geometry, and the results of a previous study of slab geometry. For the Peloponnese sector, moment tensors reaching 80 km depth were inverted, and the slab stresses were compatible with a possible slab tear. For the Kithira-Western Crete and Crete sectors, homogeneity was observed at depths up to 100 and 80 km, respectively. For these two areas, the subvertical σ_3 and along-strike σ_1 justify slab rollback as the driving mechanism. The differences in the stress regime and azimuth of the maximum compression of these two sectors may reflect a bulge in the slab. For the fourth sector, Karpathos-Rhodes, two distinct subsectors were defined along a depth gradient (50–90 km and 90–180 km, respectively). The strong heterogeneity observed at both depths and changes in the stress regime from slab pull to extension may be an indication of a double Wadati-Benioff zone. The membrane strain model presented here can provide a possible explanation for the along-strike compression observed at the top 90 km in three of the four sectors.

Key words: Slab stress, Greece, Aegean, subduction.

1. Introduction

The Southern Aegean is located on the convergent boundary of two tectonic plates, namely, the Eurasian and African plates (e.g., Jackson and McKenzie, 1988) (Fig. 1). A Wadati-Benioff zone (WBZ) identified by seismicity down to a depth of 150–180 km, is created by the subduction of the African lithosphere at a rate of about 1 cm/year and the motion of the upper Aegean plate towards the SW at a rate of 3.3 cm/year (e.g., Reilinger *et al*., 2006; Rontogianni, 2010). Seismic tomography data show that the subducting lithosphere can be traced down to about 1200 km (e.g., Bijwaard and Spakman, 1998). Several investigators have attempted to explain the complicated stress patterns present in the Hellenic subduction zone, but the limited data available to date has frustrated all such attempts to define a clear model. Kiratzi and Papazachos (1995) examined the deformation caused by 12 intermediate-depth earthquakes (40–100 km). On the basis of seismicity and moment tensor data, they showed that the angles at which T-axes dip to the inner side of the Hellenic arc are generally steeper than that of the slab dip. The P-axes appeared to be more variable and almost horizontal (6°–10°), parallel to the strike of the arc. Benetatos *et al*. (2004) used 22 intermediate-depth focal mechanisms and concluded that the distribution of T-axes shows shortening roughly parallel to the arc. The P-axes followed the trend of the arc in the eastern part, but at the western part this was not so clear.

The aim of the study reported here was to perform stress inversion on moment tensor solutions of intermediate-depth earthquakes (50 km $\leq$ depth $\leq$ 180 km). The stress field parameters were determined along the arc for several depth ranges. The slab was first divided into sectors, each containing a sufficient number of focal mechanisms for stress inversion to be performed successfully, and then subduction-related seismicity (40 km $\leq$ depth $\leq$ 180 km) was identified for each segment using data selected from global and local seismic catalogs. The results provide an updated view of the geometry for the Hellenic WBZ. The main issues addressed in this study are: (1) How does the slab stress vary horizontally and vertically along this large curvature arc? (2) Which mechanisms, as inferred from global observations, can explain this stress pattern?

2. Data

For the purposes of this study we created two catalogs: (1) a database of intermediate-depth fault mechanisms and (2) a database of intermediate-depth earthquake activity recorded up to June 2010. We collected data from various published studies as well as from global catalogs available through the World Wide Web. In order to avoid any interplate interaction for the selected moment tensors, we set the shallowest depth to 50 km; for the second catalog, depth was set to 40 km.

The first catalog contained reported data from local, regional, and global networks and covered different time intervals. Non-uniform methods were used to determine the fault plane solutions (the reader is referred to each study or

doi:10.5047/eps.2010.11.011

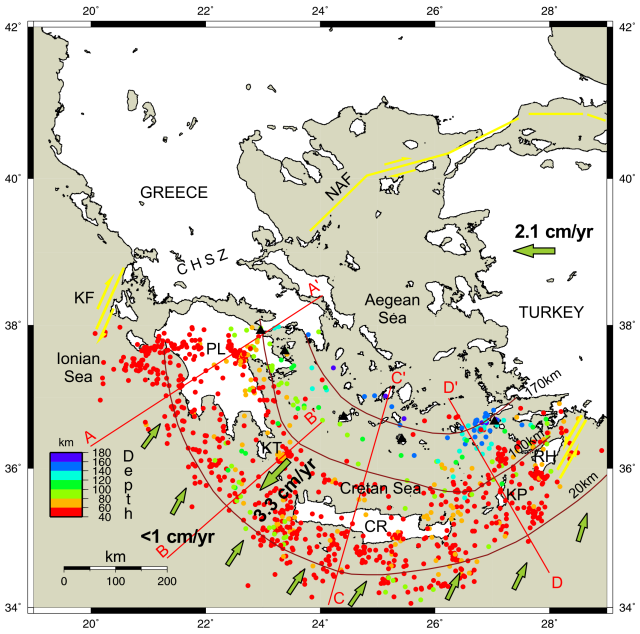

Fig. 1. Map of the Greek region showing the epicenters of the intermediate depth earthquake activity. Continuous red lines indicate the cross-sections described in Fig. 2. The thick green arrows indicate the plate motion direction along with average rate of convergence per year after Reilinger *et al*. (2006). The black triangles are the active volcanoes. The dark red curves for 20, 100 and 170 km are isodepth curves showing the hypocentral depth distribution of earthquakes occurring along the Wadati-Benioff zone. PL: Peloponnese, CR: Crete island, KP: Karpathos island, KT: Kithira island, RH: Rhodes island, KF: Kefalonia Fault, and NAF: North Anatolian Fault, CHSZ: Central Hellenic Shear Zone. (for a color version of the figure the reader is referred to the online version of the article).

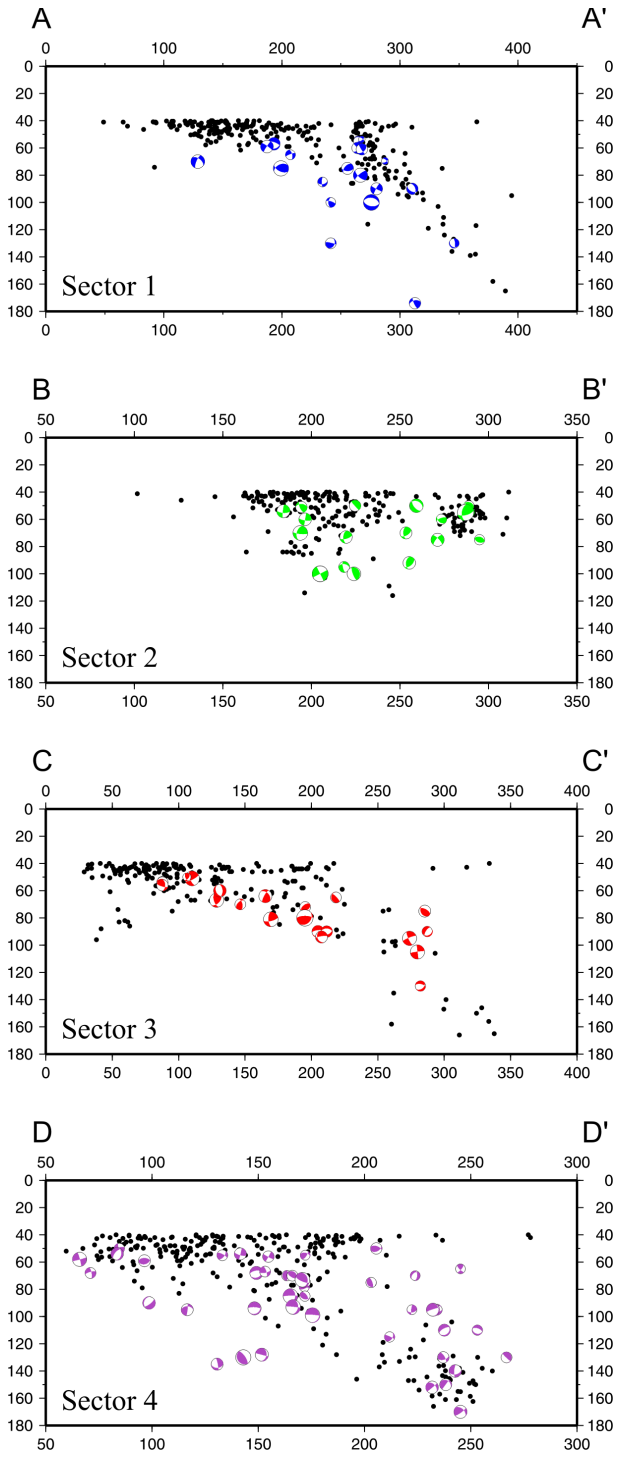

Fig. 2. Cross-sections of the earthquake foci along the subduction zone for each of the four sectors-domains shown in Fig. 1. A–A′ Peloponnese, B–B′ Kithira-Western Crete, C–C′ Crete, D–D′ Karpathos and Rhodos. The moment tensors for each domain used for stress inversion are presented along the profiles. (for a color version of the figure the reader is referred to the online version of the article).

web page). For this reason, we applied quality control criteria during the selection of the events when it was not done in the original study. The final catalog included 100 moment tensors, the largest ever dataset selected and used for stress inversion in the Hellenic area to date. We used the Engdahl *et al*. (1998) locations for any of the 100 events that could be found in the Engdahl global relocation database.

The sources for the database of the fault plane solutions, the quality criteria, and the number of events selected were:

- The National Observatory of Athens (NOA) database, from which 52 events were selected. The 41 solutions between 2001 and 2006 are included in Konstantinou *et al*. (2010); the 11 solutions for the period after 2006 are available at http://bbnet.gein.noa.gr/NOA_HL. The inversion procedure as well as the quality characterization of focal mechanism solutions based on average misfit and compensated linear vector dipole (CLVD) amount are described in Konstantinou *et al*. (2010). The selected events had an average waveform misfit smaller than 0.5 and an average CLVD of approximately 40%.
- Bohnhoff *et al*. (2005), from which nine mechanisms were selected, namely, only the most reliable as described by Bohnhoff *et al*. (2005).
- Benetatos *et al*. (2004), from which six solutions were selected. Quality control had been performed by the authors of the original study, and the earthquake source parameters had a maximum error $<30^{\circ}$.
- Global CMT catalog (http://www.globalcmt.org/CMTsearch.html), from which 15 solutions were included. The quality of these solutions was determined based on the criteria proposed by by Frohlich and Davis (1999).
- MEDNET INGV database (http://mednet.rm.ingv.it/

Table 1. Summary of stress inversion results for the different sectors mentioned in the text. For each stress axis (σ_1, σ_2, σ_3) the resulting azimuth and plunge is given along with the value of R and the misfit angle $\overline{\beta}$. Total MT is the number of all the available focal mechanisms in each sector, N is the number of focal mechanisms used in each stress inversion.

Sector	Depth (km)	Total MT	N	σ_1 azimuth/plunge (°)	σ_2 azimuth/plunge (°)	σ_3 azimuth/plunge (°)	R	$\overline{\beta}$
1	50–80	20	12	231/57	327/4	59/33	0.4	47
2	50–100	18	18	167/12	262/21	47/66	0.3	33
3	50–80	20	12	263/6	355/17	154/72	0.6	31
4	50–90	42	23	200/7	102/48	297/42	0.5	49
	90–180		19	173/46	64/17	320/39	0.3	51

rcmt.php), from which nine events were selected. Only events with quality flag A–B were accepted.

- SED (ETH Zürich) database (http://www.seismo.ethz.ch/prod/tensors/index_EN), from which four events were selected. Only events with quality A were accepted.
- EMMA database (Vannucci and Gasperini, 2004 (http://gaspy.df.unibo.it/paolo/ATLAS/pages/EMMA_READ_ME.html)), from which five events were selected.

For each segment we identified subduction-related seismicity using data from three sources:

- For moderate-to-large events ($M > 5.5$), the locations are constrained from the global relocation database of Engdahl *et al*. (1998) and its subsequent updates that extend throughout 2005.
- For smaller events ($M \sim 3.5$), locations are taken from Papazachos *et al*. (2000).
- For events after 2006 and up to 31 May 2010 we used the NOA database (http://bbnet.gein.noa.gr/NOA_HL). The selection criteria here was (1) the event had to have been recorded by more than four stations and (2) the depth error had to be <5 km. The final catalog included more than 1100 events (Fig. 1).

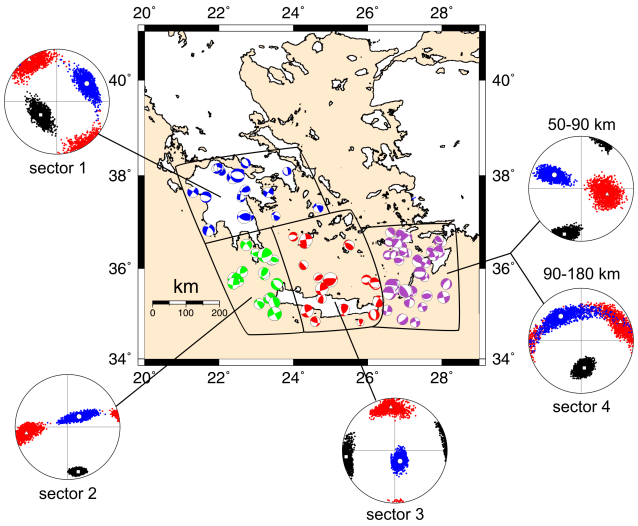

Fig. 3. Map view of the distribution of the 100 focal mechanisms used in this study. The different color of the beach balls indicates the different sectors, blue—Peloponnese, green—Kithira-Western Crete, red—Crete, purple—Karpathos-Rhodos. For each sector we present lower hemisphere projections of the directions of the principal stress axes obtained from the datasets listed in Table 1 (see also text for more details). The square represents the σ_1 axis, the circle signifies the σ_3 and the triangle the σ_2 axis. The colored dots define the 68% confidence region of each stress axis. (for a color version of the figure the reader is referred to the online version of the article).

3. Stress-Inversion Methodology

In order to study and evaluate the stress regime of the Hellenic WBZ, we applied the inversion technique of Michael (1987) to the earthquake focal mechanism catalog. The technique is not discussed here in detail, but the interested reader is referred to the articles of, for example, Michael (1987, 1991) and Hardebeck and Hauksson (2001). The algorithm uses the statistical method of bootstrap resampling and allows the three principal stresses (σ_1 = maximum, σ_2 = intermediate, σ_3 = minimum) to be determined as well as a relative stress magnitude $R = (\sigma_1 - \sigma_2)/(\sigma_1 - \sigma_3)$, $0 < R < 1$. The method also calculates the misfit between the best fit model and the data given by $\overline{\beta}$, the angle between the slip direction and the predicted tangential traction on the fault plane. Michael (1991) estimated the variation of $\overline{\beta}$ as a function of the standard deviation of the errors in strike, dip, and rake of the fault plane solutions (FPS). For FPS errors varying from 10 to 25°, the misfit angle can range from 30 to 45° (Michael, 1991), indicating that stress inversion results with misfits lower than this are considered acceptable and that the stress field is approximately homogeneous.

In order to divide the Hellenic subduction zone into sectors, we made use of all available information from previous studies that used different methods to investigate the slab. We divided our sectors on the basis of earthquake distribution, trench geometry, and results from earlier studies on slab geometry (Papazachos and Nolet, 1997; Konstantinou and Melis, 2008). We then applied the inversion method with the objective of using the maximum number of available focal mechanisms and including depths close to 180 km in the analysis. However, this was not possible since only one of the four sectors had a sufficient number (>12) focal mechanisms for depths below 90 km. Table 1 lists the number of input datasets, the depth ranges for each sector, the directions of the three principal stresses, the R value, and the average misfit $\overline{\beta}$. Profiles of the WBZ along each domain were plotted to examine their shape and geometry (Fig. 2). The best fit stress solutions and 68% confidence limits obtained by the inversion are presented as lower hemisphere projections in Fig. 3.

4. Results

4.1 Sector 1: Peloponnese

Stress inversion was applied to focal mechanisms at depths ranging from 50 to 80 km, leading to an acceptable misfit (∼47°). The misfit level shows that a small level of heterogeneity is present in the stress regime that might be caused by pre-existing faults of different orientation. The value of R is 0.45, suggesting that the stress regime is triaxial. The best stress model has a maximum compression σ_1 trending 231° and is almost normal to the slab (dip ∼ 57°), while the minimum compression σ_3 dips at 33° (Fig. 3). The minimum compression appears to be steeper than the slab if we accept a slab dip of around ∼30°, as suggested by Papazachos *et al.* (2000) or ∼21°, as reported by Suckale *et al.* (2009) (determined by backscattered P- and backscattered S_h-waves). The σ_3 axis follows the slab if we accept a slab dip of ∼34° (apparent only on the S-mode images of the northern back azimuths in the Suckale *et al.* (2009) study). The dipping directions of the σ_1 and σ_3 axes suggest that the slab plane is under extension. If the σ_3 axis is steeper than the slab, a component of slab-pull force is unbalanced by the subduction resistance. This unbalanced slab-pull force has been described by Scholz and Campos (1995) as the trench suction force, which contributes to the seismic decoupling at the plate interface. If we accept a σ_3 axis along the slab, then no suction force is required.

4.2 Sector 2: Kithira-Western Crete

The focal mechanisms that gave well-constrained stress directions and a homogeneous stress field (acceptable misfit ∼30°) ranged in depth from 50 to 100 km. There were no available focal mechanisms below this depth. The orientation of the σ_1 axis changes significantly when compared to that of Sector 1 and is almost along the strike (dip ∼ 12°) trending 167° (Fig. 3). The stress regime is biaxial, i.e., of confined extension ($R = 0.3$).

4.3 Sector 3: Crete

In this sector fewer than 12 events below a depth of 80 km were available for stress inversion estimation at two depth ranges. Papazachos *et al.* (2005) suggested that the lack of seismicity at depths between 90 and 140 km is a result of the high temperature, an indication that the primary magma in southern Aegean is located in the asthenospheric wedge between the descending Mediterranean and the overriding Aegean microplates under the volcanic arc. The best solution was given for depths between 50 and 80 m. The model misfit is around 30°, indicating a homogeneous stress field. The maximum compression is oriented, as in sector 2, along the strike (dip ∼ 6°). The minimum compression σ_3 is almost subvertical to the slab orientation (dip ∼ 71°) (Fig. 3). The stress regime shows confined compression ($R \approx 0.6$).

4.4 Sector 4: Karpathos and Rhodes

Applying the stress inversion for the whole depth range (50–180 km) resulted in a misfit of >45°, implying that the stress field is probably heterogenous and cannot be described by a single stress tensor. We divided this sector in two depth ranges: 50–90 km and 90–180 km, respectively. The shallow subset (50–90 km) shows a σ_1 almost along the strike (dip ∼ 7°) and σ_3 shows a down dip (dip ∼ 42°) (Fig. 3), implying the presence of slab-pull forces. R has a value of around 0.5, suggesting that the stress regime is triaxial. The deeper subset (90–180 km) has a different stress regime, with the σ_1 slab vertical and σ_3 parallel to the slab. R has a value of 0.3, suggesting that the stress regime is biaxial, i.e., of confined extension. For both depth ranges of this sector, the high inversion misfit points to the possibility that not a single stress tensor can describe the stress conditions within the slab.

5. Discussion

The results determined from the stress tensor inversion underline the complexity surrounding the strongly curved Hellenic arc. The Peloponnese segment is under an extension regime, but the way the slab-pull force is expressed, i.e., in balance or not with the subduction resistance, depends on the accepted dip for the slab. The stress inversion results derived for this sector support the concept of a possible N-S oriented slab tear beneath the Peloponnese. The slab tear model has been also observed in a number of different subduction zones (e.g., Miyoshi and Ishibashi, 2005). Meijer and Wortel (1996) used numerical modeling to suggest that the tip of the tear migrated southwards over time, and their model currently extends the detachment tear to a point in the southern Peloponnese. Suckale *et al.* (2009) obtained high-resolution two-dimensional images of the subduction zone by deploying a temporary array of densely spaced broad-band seismometers that crossed the Peloponnese (from SW ∼ 21.6°E, 37.2°N to NE ∼ 24.5°E, 38.8°N). These researchers also inferred a possible tear in the slab directly north of their array below the Central Hellenic Shear Zone-CHSZ (see Fig. 1).

For the second (Kithira-Western Crete) and third segment (Crete), the σ_1 axis is along the strike, and σ_3 is almost subvertical to the slab. The orientation of σ_3 unbalances the slab-pull force (negative buoyancy of the slab), which induces a vertical velocity on the slab and, most importantly, reduces the normal force acting on the plate interface, leading to slab rollback (Scholz and Campos, 1995). The results from previous studies have supported similar patterns for the intermediate-depth events in this region of the slab. Bohnhoff *et al.* (2005) also determined a subvertical orientation for σ_3 (dip ∼ 70°) for this area, adding that slab pull is the dominant force within the subduction process and responsible for the roll-back of the Hellenic subduction zone. Stress inversion was initially performed on these two sectors together but led to a rather large misfit. The details of the stress regime differ for the two sectors, with confined extension present for the second sector, turning to confined compression for the third. The azimuth of the maximum compression for the second sector has an almost N-S direction; this has an E-W direction for the third sector. These observed differences in the stress regime may reflect a change in the slab's curvature between Kithira and Crete, possibly a bulge or folding in the slab. Such a bulge has been observed in western Crete at around a depth of 60 km using teleseismic receiver functions (Knapmeyer and Harjes, 2000).

The stress field for the fourth segment—that below Karpathos and Rhodes—has been divided into two depth ranges. The shallow part is characterized by slab-pull forces. The deeper subset shows that the σ_1 slab is nor-

mal and that σ_3 is parallel to the slab, indicating an extension regime. In this sector, strong heterogeneity is expressed at both depths by the large $\overline{\beta}$. Double WBZs have been observed in various subduction zones where the stress state of the slab changes from top to bottom (Kawakatsu and Seno, 1983). In the same manner, this stress regime, which changes from a simple slab pull to extension, might be interpreted by the presence of a DWBZ. The observed heterogeneity may be the result limitations in the dataset. In general, DWBZs have been described in areas where local seismic networks provide sufficient coverage to determine high-resolution earthquake locations. It is possible, therefore, that the lack of high-resolution locations along the Hellenic subduction zone hides the existence of a DWBZ and leads to the observed heterogeneity in sector 4. Two types of stress fields have been identified in the Nankai subduction zone (Xu and Kono, 2002); these have been explained by differences in the geometry and age of the subducting zone.

The along-strike maximum compression observed in sectors 2, 3, and 4 (top 90 km) can be explained by the "tablecloth effect" or membrane strain model (e.g., Creager *et al.*, 1995). According to this model, the slab geometry is analogous to a table cloth draped over the corner of a table, producing a slab with too much material (pleats in the table cloth) to fit around the corner, developing compressive along-strike membrane strains or geometric buckling. More data are needed in terms of precise earthquake locations and moment tensor solutions in order to shed light on the finer details of the slab's geometry and stress variations along the Hellenic arc.

6. Conclusions

The main conclusions that can be drawn from this study are:

1. The Hellenic subduction zone can be divided from west to east into four sectors based on differences in the stress regime, slab geometry, earthquake depth distribution: (1) Peloponnese; (2) Kithira-Western Crete; (3) Crete; (4) Karpathos-Rhodes.
2. The slab stresses in the Peloponnese sector are related to slab-pull forces and are consistent with a possible tear in the slab below this segment.
3. For the second and third sectors, slab rollback is the mechanism able to explain the observed stress distribution, with the minimum compression almost subvertical to the slab.
4. The differences in the relative stress magnitude and orientation of the σ_1 axis between the Peloponnese-Kithira strait and western Crete may reflect changes in the slab's curvature.
5. The Karpathos-Rhodes area showed two distinct stress states for the top and lower depth ranges. The shallow part is characterized by slab-pull forces and the lower part showed a general extension regime. However, what is more prominent is the presence of stress heterogeneity expressed at both depths. A masked DWBZ might be able to explain this prominent heterogeneity and the stress regime that changes from a simple slab pull to an extension regime.

Acknowledgments. This research was supported by the National Science Council (NSC) of Taiwan. The first author also holds a postdoctoral fellowship funded by the NSC of Taiwan.

References

Benetatos, C., A. Kiratzi, C. Papazachos, and G. Karakaisis, Focal mechanisms of shallow and intermediate depth earthquakes along the Hellenic Arc, *J. Geodyn.*, **37**, 253–296, 2004.

Bijwaard, H. and W. Spakman, Closing the gap between regional and global travel time tomography, *J. Geophys. Res.*, **103**, 30055–30078, 1998.

Bohnhoff, M., H.-P. Harjes, and T. Meier, Deformation and stress regimes in the Hellenic subduction zone from focal mechanisms, *J. Seismol.*, **9**, 341–366, 2005.

Creager, K. C., L.-Y. Chiao, J. P. Winchester, and E. R. Engdahl, Membrane strain rates in the subducting plate beneath South America, *Geophys. Res. Lett.*, **22**, 2321–2324, 1995.

Engdahl, E. R., R. van der Hilst, and R. Buland, Global teleseismic earthquake relocation with improved travel times and procedures for depth determination, *Bull. Seismol. Soc. Am.*, **88**, 722–743, 1998.

Frohlich, C. and S. D. Davis, How well are well-constrained T, B and P axes in moment tensor catalogs?, *J. Geophys. Res.*, **104**, 4901–4910, 1999.

Hardebeck, J. L. and E. Hauksson, Stress orientations obtained from Earthquake focal mechanisms: What are appropriate uncertainty estimates?, *Bull. Seismol. Soc. Am.*, **91**, 250–262, doi:10.1785/0120000032, 2001.

Jackson, J. and D. P. McKenzie, The relationship between plate motion and seismic moment tensors, and the rates of active deformation in the Mediterranean and Middle East, *Geophys. J. Int.*, **93**, 45–73, 1988.

Kawakatsu, H. and T. Seno, Triple seismic zone and the regional variation of seismicity along the northern Honshu arc, *J. Geophys. Res.*, **88**, 4215–4230, 1983.

Kiratzi, A. A. and C. B. Papazachos, Active deformation of the shallow part of the subducting lithospheric slab in the southern Aegean, *J. Geodyn.*, **19**, 65–78, 1995.

Knapmeyer, M. and H.-P. Harjes, Imaging crustal discontinuities and the downgoing slab beneath western Crete, *Geophys. J. Int.*, **143**, 1–21, 2000.

Konstantinou, K. I. and N. S. Melis, High-frequency shear-wave propagation across the Hellenic subduction zone, *Bull. Seismol. Soc. Am.*, **98**, 797–803, doi: 10.1785/0120060238, 2008.

Konstantinou, K. I., N. S. Melis, and K. Boukouras, Routine regional moment tensor inversion for earthquakes in the Greek region: The National Observatory of Athens (NOA) database (2001–2006), *Seismol. Res. Lett.*, **81**, 750–760, doi:10.1785/gssrl.81.5.738, 2010.

Meijer, P. T. and M. J. R. Wortel, Temporal variation in the stress field of the Aegean region, *Geophys. Res. Lett.*, **23**, 439–442, 1996.

Michael, A. J., Use of focal mechanisms to determine stress: A control study, *J. Geophys. Res.*, **92**, 357–368, 1987.

Michael, A. J., Spatial variations in stress within the 1987 Whittier Narrows, California, aftershock sequence: New techniques and results, *J. Geophys. Res.*, **96**, 6303–6319, 1991.

Miyoshi, T. and K. Ishibashi, A tectonic interpretation of the NW-SE strike-slip faulting during the 2004 off the Kii peninsula earthquakes, Japan: Probable tear of the Philippine Sea plate, *Earth Planets Space*, **57**, 1115–1120, 2005.

Papazachos, C. and G. Nolet, P and S deep velocity structure of the Hellenic area obtained by robust nonlinear inversion of travel times, *J. Geophys. Res.*, **102**, 8349–8367, 1997.

Papazachos, B. C., V. G. Karakostas, C. B. Papazachos, and E. M. Scordilis, The geometry of the Wadati-Benioff zone and lithospheric kinematics in the Hellenic arc, *Tectonophysics*, **319**, 275–300, 2000.

Papazachos, B. C., S. T. Dimitriadis, D. G. Panagiotopoulos, C. B. Papazachos, and E. E. Papadimitriou, Deep structure and active tectonics of the Southern Aegean volcanic arc, in *Developments in Volcanology: The south Aegean Volcanic Arc*, edited by M. Fytikas and G. Vougioukalakis, 47–64, 391 pp, Elsevier, Amsterdam, 2005.

Reilinger, R. *et al.*, GPS constraints on continental deformation in the Africa-Arabia-Eurasia continental collision zone and implications for the dynamics of plate interactions, *J. Geophys. Res.*, **111**, B05411, doi:10.1029/2005JB004051, 2006.

Rontogianni, S., Comparison of geodetic and seismic strain rates in Greece by using a uniform processing approach to campaign GPS measurements over the interval 1994–2000, *J. Geodyn.*, **50**, 381–399, doi:10.1016/j.jog.2010.04.008, 2010.

Scholz, C. H. and J. Campos, On the mechanism of seismic decoupling and back arc spreading at subduction zones, *J. Geophys. Res.*, **100**, 22103–22115, 1995.

Suckale, J., S. Rondenay, M. Sachpazi, M. Charalampakis, A. Hosa, and L. H. Royden, High-resolution seismic imaging of the western Hellenic subduction zone using teleseismic scattered waves, *Geophys. J. Int.*, **178**, 775–791, doi: 10.1111/j.1365-246X.2009.04170.x, 2009.

Vannucci, G. and P. Gasperini, The new release of the database of Earthquake Mechanisms of the Mediterranean Area (EMMA Version 2), *Ann. Geof., Suppl*, **47**, 307–334, 2004.

Xu, J. and Y. Kono, Geometry of slab, intraslab stress field and its tectonic implication in the Nankai trough, Japan, *Earth Planets Space*, **54**, 733–742, 2002.

S. Rontogianni (e-mail: sofia@ncu.edu.tw), K. I. Konstantinou, N. S. Melis, and C. P. Evangelidis